electronics

MDPI

Article

Reflection Suppression through Modal Filtering for Wideband Antenna Measurement in a Non-Absorbent Environment

Yao Su * and Shuxi Gong

School of Electronic Engineering, Xidian University, Xi'an 710071, China
* Correspondence: yaosu.xdu@hotmail.com

Abstract: In order to reduce the influence of multi-path effects on the measurement results of wideband antennas, this paper proposes a method for suppressing interference in wideband antenna measurements based on modal filtering technology. This paper introduces the theory and operation process of modal filtering, establishes the relationship between the distribution of modal coefficient terms and the location of the antenna and external interference sources, and clearly reveals the principle of filtering interference through modal filtering. It is pointed out that each location of interference sources corresponds to different pattern items. Filtering out the power of the pattern term generated by the interference source is equivalent to filtering out the interference caused by the interference source. The sources filtered by this technology are external sources that are spatially separated from the antenna, including external sources, environmental reflections, and device reflections, among others. This feature makes it possible to be used for testing in a non-absorbent environment. Its ability to operate at almost any frequency makes it ideal for suppressing interference effects in wideband antenna measurement. This paper demonstrates a recent advance wherein modal filtering techniques are used in interference suppression for wideband antenna non-absorbent measurement. In the full bandwidth range of the wideband antenna, we verify the method through numerical simulation analysis and practical measurement. In the numerical simulation, we obtain that 15 dB interference can be filtered out at the −25 dB level and 5 dB interference can be filtered out at the −35 dB level. In the experiments, within the broadband antenna bandwidth, we found that 2.5 dB can be filtered at the −10 dB level at 4 GHz, 3 dB is filtered at the −10 dB level at 6 GHz, and 5 dB is filtered at the −10 dB level at 7.5 GHz. All of the above results prove that the proposed method can effectively suppress the multi-path interference in wideband non-absorbent antenna measurement and improve the measurement results.

Keywords: modal filtering; antenna measurement; spherical wave expansion; reflection suppression

check for updates

Citation: Su, Y.; Gong, S. Reflection Suppression through Modal Filtering for Wideband Antenna Measurement in a Non-Absorbent Environment. *Electronics* **2022**, *11*, 3422. https://doi.org/10.3390/electronics11203422

Academic Editor: Raed A. Abd-Alhameed

Received: 24 September 2022
Accepted: 19 October 2022
Published: 21 October 2022

1. Introduction

Wideband antenna is a common antenna, widely used in all aspects of production and life. In wideband antenna measurement, the error source mainly comes from the interference of external radiation sources and a non-ideal test environment [1], such as reflection from walls, floors, ceilings, and field equipment. The existence of multi-path effects in the measurement mainly affects the measurement accuracy of the low sidelobe of the wideband antenna [2].

Usually, absorbing materials are used to shield the site and equipment to simulate free space without reflection. However, there are inevitably some parts in the measurement site that cannot be laid with absorbing materials, such as antenna brackets and probe scanning frames, among others. At the same time, the size and shape of the absorbing material determine that the absorbing performance of the absorbing material is only optimal in some specific frequency bands, but not optimal in other frequency bands, and its absorbing effect will deteriorate over time. Therefore, it is of great significance to reduce the multi-path interference by applying modal filtering in the non-absorbent measurement environment.

For the above problems, a modal filtering technique [3–5] based on spherical wave expansion theory is proposed, which can effectively suppress external source interference and the multi-path effect interference in measurement [6]. In order to reduce the influence of the multi-path effect, in addition to the modal filtering method, time gating technology and background subtraction can also play a role. I have presented the Table 1 comparing the three methods for reflection suppression in wideband antenna measurements. Time gating technology uses the difference in the arrival time of the radiation signal and the interference signal at the receiver; the radiation signal is intercepted through the time gate, so as to shield the interference signal. It requires large bandwidths of the measurement setup and the antenna under test (AUT) for a sufficient temporal resolution, especially for reflections that occur close to the AUT. Large signal bandwidth is required to obtain a high resolution in the time domain, and multi-path elimination is difficult to achieve at a low frequency (P and L band). As for the background subtraction, the dual-channel receiver is used to obtain the environment level signal and the measurement level signal at the same time, and the background noise interference caused by the environment signal is filtered out by the algorithm. Background subtraction requires additional measurements and data acquisition. It is suitable for an insufficient frequency band, generally less than 18 GHz.

Table 1. Comparison of different methods. N is the quantity of frequencies required.

	Modal Filtering Method	**Time Gating Technology**	**Background Subtraction**
Number of measurements required	1	N	N
Frequency range of application	No limit to frequency	Low frequency (P and L band) is not applicable	Less than 18 GHz
Efficiency	Test all frequencies in the band	Test one frequency in one test	Test one frequency in one test
Testing environment	Non-absorbent environment or absorbent environment	Absorbent environment	Absorbent environment

Modal filtering is a post-processing technique that involves analysis of the measured data and a special modal filtering process to suppress the undesirable scattered signals. At present, this method has been used in an anechoic chamber with a pyramidal absorber and absorber baffles that cover all of the floors and walls. It is shown that modal filtering is applicable in spherical [7,8], cylindrical [9,10], and planar [11,12] near-field antenna measurement systems, as well as in the measurement of some feeding integrated antennas working at high frequencies [13,14], which effectively reduces the interference from the environment. It only needs the amplitude and phase data of the radiated field strength of the AUT and the maximum radial extent (MRE) surrounding the AUT. In this case, the MRE is defined as the radius of a conceptual sphere centred about the origin of the measurement coordinate system, and that is sufficiently large to encompass the majority of the current sources. Only a single measurement is needed to obtain the accurate field distribution after interference suppression from the results of interference with multi-path effects after processing by modal filtering. The modal filtering technique has no limit to the working frequency in theory and is suitable for the measurement of a wideband antenna environment, such as Vivaldi antenna measurement [15,16]. In the following, we introduce the typical improvements to modal filtering in a non-absorbent environment from the aspects of numerical simulation and experimental verification.

2. Theoretical Basis of Modal Filtering

The far-field pattern of the antenna is different in different coordinate systems, so it is necessary to perform coordinate translation first. The origin of the coordinate system is translated to the center of the antenna mouth according to the actual measurement position. Different coordinate systems only affect the phase pattern, not the amplitude [17]:

$$\boldsymbol{E}(\theta,\varphi) = \boldsymbol{E_m}(\theta,\varphi)e^{jk(\boldsymbol{r'}\cdot\hat{r})} \tag{1}$$

where k is the wave number, $\boldsymbol{r'}$ is the vector of the origin of the original coordinate system pointing to the center of the radiating element to be calculated, and $\hat{r}$ is the unit vector.

The electric field E radiated from a source of finite range can be expressed as a superposition of spherical waves [18]:

$$\boldsymbol{E}(r,\theta,\varphi) = \frac{k}{\sqrt{\eta}}\sum_{s=1}^{2}\sum_{n=1}^{N}\sum_{m=-n}^{n} Q_{smn}\boldsymbol{F}_{smn}(r,\theta,\varphi) \tag{2}$$

The field is fully characterised by the modal coefficients Q_{smn} to the spherical wave functions $\boldsymbol{F}_{smn}(r,\theta,\varphi)$. The order m is limited by $|m| \leq n$ and the degree n is limited by the extent of the sources. The index s takes on the value 1 for TM fields and 2 for TE fields.

The field of the antenna contains infinite terms. Let the minimum spherical radius surrounding the antenna under test be r_0. Generally, only the term $N = k \times r_0$ contributes greatly to the far field of the antenna. From a practical point of view, the number of truncated modes of the spherical wave function [19] can be expressed as

$$N = [k \times r_0] + n \tag{3}$$

Among them, $[k \times r_0]$ represents the nearest integer of $k \times r_0$. The size of n is adjusted according to the coordinate position and precision, usually selecting $n = 10$. After modal filtering, the multi-path interference in the environment can be filtered out.

The spherical wave functions are power-normalized such that the power of the radiated field [20] given by Equation (2) is

$$P_{rad} = \frac{1}{2}\sum_{smn}|Q_{smn}|^2 \tag{4}$$

We define P_n as the power spectrum in n [20]

$$P_n = \frac{1}{2}\sum_{sm}|Q_{smn}|^2 \tag{5}$$

For a truncation of the modes at $t \leq N$, the sum of the power spectrum from 1 to N is the truncation power P_t

$$P_t = \sum_{n=1}^{t} P_n \tag{6}$$

Therefore, by measuring the far-field amplitude and phase of the antenna, the power of the spherical wave modes of each order n can be obtained. By filtering the power spectrum according to the minimum sphere radius surrounding the antenna, the antenna pattern after filtering out multi-path interference can be obtained.

3. Simulation Experiment

In order to reveal the principle of the modal filtering technique more clearly, we start with the spherical wave expansion of the antenna radiated electric field. With the help of the commercial simulation software FEKO, the distribution law of the spherical mode term coefficients (SMCs) of the standard gain horn (SGH) model working in the S-band was analyzed, and a metal plate was placed as an interfering object to simulate the multi-path effect interference during the measurement process.

The schematic diagram of the simulation model is shown in Figure 1 below, using Cartesian coordinates. The phase center(O1) of the standard gain horn is located at the origin(O) of the coordinate system of the measurement system. The XOY plane of the coordinate axis is parallel to the antenna aperture plane and the maximum radiation direction is along the Z axis. The metal plate has a size of 200 mm × 200 mm; its four sides are parallel to the coordinate axis; the surface is parallel to the antenna aperture surface; and its center (O2) is located at (0, 625 mm, 625 mm), which simulates the interference objects that cause multi-path effects in the measurement field.

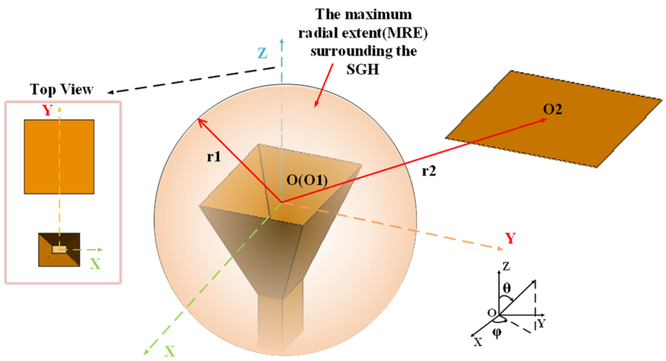

Figure 1. Antenna model with the metal plate.

The two models of the absence and presence of the metal plate in Figure 1 are analyzed respectively. Taking the phase center of the horn as the origin and the minimum spherical radius surrounding the horn antenna as r1 = 198 mm (1.587λ1), λ1 = 125 mm, only N1 = [k × r1] = 10 mode items are needed to characterize the radiation characteristics of the entire horn. The SGH radiation field data at the frequency of 2.4 GHz are used. According to the aforementioned spherical wave expansion method of the electric field, the SMC of each mode item is used to calculate the power contained in the mode item. The resulting power spectrum distribution is shown in Figures 2 and 3 below.

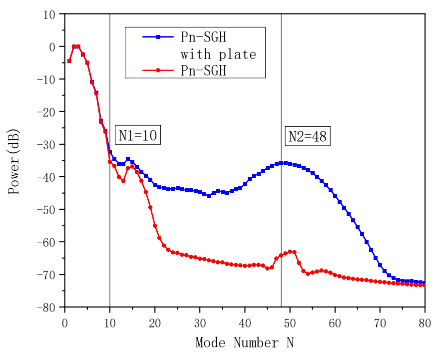

Figure 2. Comparison of the power spectrum distribution of the model with the presence of the plate and the model without the presence of the plate.

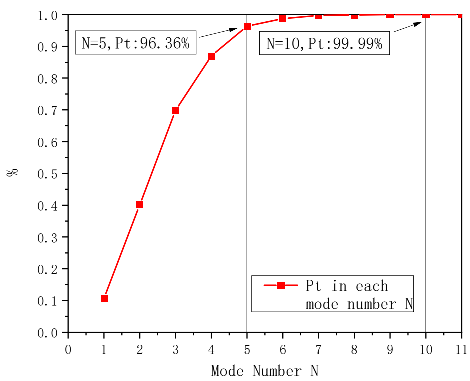

Figure 3. Distribution of the first N sums of the power spectrum of a single horn antenna.

The power spectrum distribution curve of the single horn antenna model in Figure 2 shows that the radiated power of SGH is mainly distributed on the low-order mode terms, and the radiated power decreases rapidly with the increase in the number of mode terms until it can be ignored. Figure 3 shows that only the first 10 terms are required to include 99.99% of the SGH radiated power. This is consistent with the selection of the first N1 = [k × r1] = 10 terms in the spherical wave mode term number truncation principle. For the SGH with the same operating frequency (2.4 GHz) and the same size, only the first 10 items of its radiation field SMCs are needed to fully express its radiation characteristics. For the power spectrum distribution of the horn antenna in the presence of the metal plate in Figure 2, the power distribution also appears in several items near the 48th item of the spherical wave mode item, and the maximum power distribution item N2 = 48 is consistent with the position of the metal plate N2 = [k × r2] = 48, where the power represents the interference of the metal plate as an interference source to the radiation field of the horn antenna. The modal filtering technology determines the number of corresponding mode items according to the spatial distribution of different field sources, and extracts the mode items corresponding to the AUT to filter out the mode items corresponding to the interference sources. That is, the influence of the interference source is filtered out from the radiation field of the AUT containing external interference, and the radiation characteristics of the AUT in which the external interference source is suppressed are obtained. The interference from the environment is effectively reduced and accurate measurement of the AUT is realized.

In the simulation of the model shown in Figure 1, the SGH radiation field data at a frequency of 2.4 GHz are also used, and the metal plate can simulate the external interference objects during measurement. The electromagnetic wave radiated by the SGH enters the measurement receiving a probe through the reflection of the metal plate, which has a significant impact on the measurement results of the antenna radiation field, resulting in obvious changes in some radiation directions, as shown in Figure 4. In this coordinate, the E-plane of the horn refers to the YOZ plane and the H-plane of the horn refers to the XOZ plane. They represent a cross section of the horn antenna radiation field, where the theta coordinate component ranges from −180° to 180°. E1 represents the horn radiation pattern when SGH exists independently, E2 represents the radiation pattern when SGH and the metal plate coexist, and E3 represents the radiation pattern after modal filtering when SGH and the metal plate coexist. In Figure 4, the black dotted curves E1 for the E-plane and E1 for the H-plane represent the cross-section radiation field intensity of radiation field E1 on the E-plane or H-plane, the red dashed curves E2 for the E-plane and E2 for the H-plane represent the cross-section radiation field intensity of radiation field E2 on the E-plane or H-plane, and the blue solid curves E3 for the E-plane and E3 for the H-plane represent the cross-section radiation field intensity of radiation field E3 on the E-plane or H-plane.

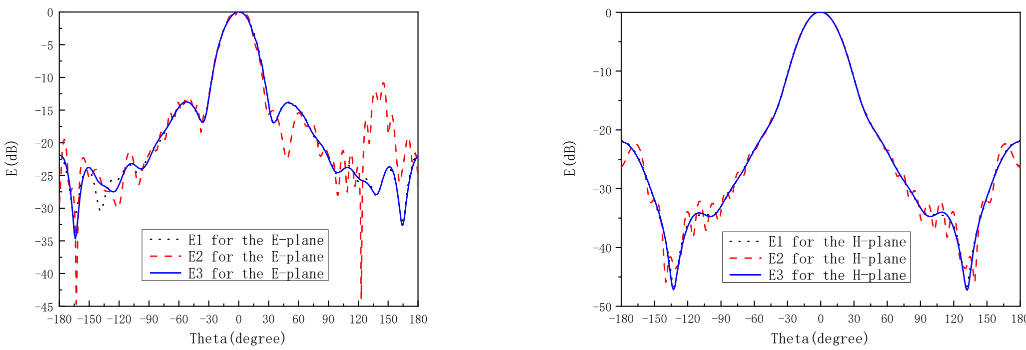

(**a**) (**b**)

Figure 4. Pattern of the H-plane of the antenna. (**a**) E-plane; (**b**) H-plane.

Comparing the black curve and the red curve, owing to the existence of the interference metal plate, as well as the superposition of the interference signal and antenna radiation signal, the red curve of the received measurement result has a large error as a whole. In the main lobe of the pattern, the interference causes the main lobe to shrink and split. On the side lobes, the interference caused is more pronounced; particularly, when the probe is at theta = 40°, the receiving probe, the center of the metal plate, and the center of the aperture surface of the horn antenna are on a line. The existence of the metal plate blocks the received signal, resulting in a significant reduction in the amplitude of the received signal and the formation of a depression. On the E-plane radiation pattern of the SGH shown in Figure 4a, the presence of the metal plate causes burrs in the side lobes of the antenna pattern. Especially, when the receiving probe is at theta = 140°, the electromagnetic wave emitted by the antenna is reflected by the metal plate mirror and directly enters the receiving probe. At this time, the reflection interference is strong, resulting in a serious bulge in the pattern of the SGH. Similarly, on the H-plane radiation pattern of the SGH shown in Figure 4b, the presence of the metal plate has almost no effect on the main lobe of the pattern, but in the area outside the main lobe, especially the side lobe position, there are obvious fluctuations and burring, resulting in measurement errors.

It can be seen from Figure 4 that the presence of the metal plate significantly affects the radiation characteristics of the measured SGH. After being processed by the modal filtering technology, the superimposed interference and occlusion interference are eliminated, and the influence of external interfering objects is suppressed. Comparing the black curve and the blue curve in Figure 4a,b, the pattern filtering technique eliminates the contraction and splitting of the main lobe, so that the corrected main lobe of the orientation pattern exactly matches the main lobe when there is no interference. On the sidelobes, the burrs and jitter caused by the interference are eliminated. In the other directions, there is a significant reduction in the variation of the orientation pattern owing to the interference. In Figure 5 below, we quantitatively calculate the degree of interference suppression using the pattern filtering technique by calculating the difference value between the pattern before and after filtering correction and the pattern without interference.

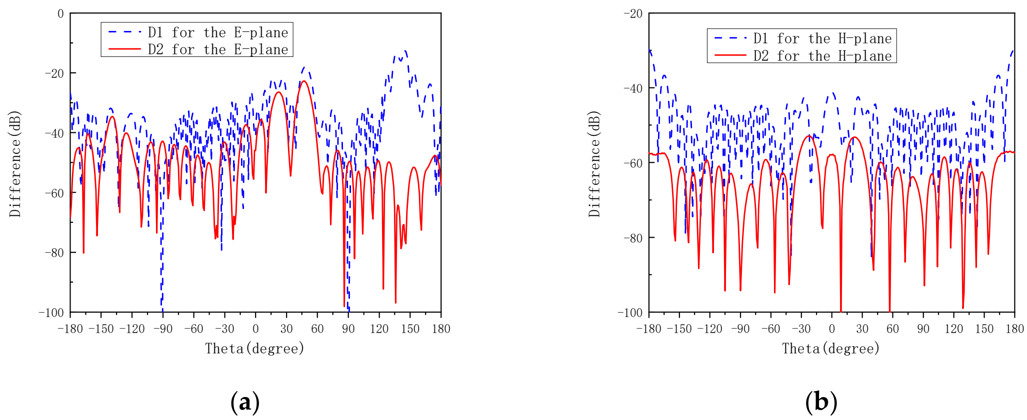

Figure 5. Comparison of the pattern. (**a**) E-plane; (**b**) H-plane.

In Figure 5, the blue dotted curve D1 for the E-plane represents the difference value D1 in the measured AUT radiation field with and without the metal plate. The red solid curve shows the difference value D2 between the field after modal filtering the field in the presence of a metal plate interferer and the radiated field from the AUT alone. At all angles, the modal filtering technology reduces the influence of the interference source on the AUT. On the E-plane of the SGH, the maximum 15 dB interference is filtered out at the −25 dB level, so that the difference between the two curves is reduced from the maximum −17 dB to −50 dB. On the H-plane of the SGH, the maximum 5 dB interference is filtered out at the −35 dB level, so that the difference between the two curves is reduced from the maximum −30 dB to −58 dB.

The above numerical simulation analysis shows that the modal filtering technology has a strong suppression effect on the external interference in the wideband antenna measurement, and can significantly improve the test accuracy of the AUT.

4. Experimental Verification

Figure 6 shows the measurement setup used to verify the above methods. In the test field, the walls and ground are partially wrapped by absorbing material and the ceiling and equipment cables are exposed, which are the main sources of multi-path interference. This measurement environment, similar to a non-absorbent environment, has strong reflection interference from itself and artificially placed interference objects.

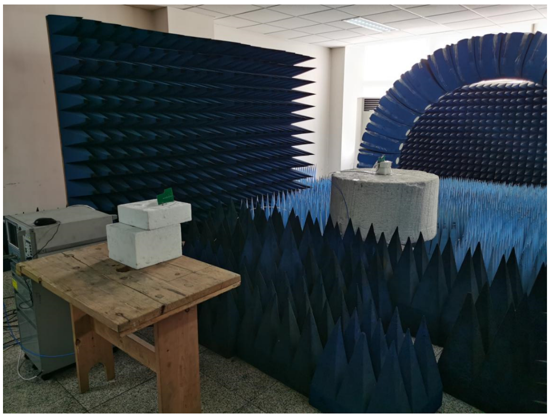

Figure 6. Testing environment with the Vivaldi antenna alone.

The antenna under test is a Vivaldi antenna, a wideband antenna with a size of 100 mm × 85 mm ($1.6\lambda 0 \times 1.4\lambda 0$), $\lambda 0$ = 60 mm, where the antenna center frequency is 5 GHz. The minimum radius of the sphere surrounding the antenna is r0 = 52.2 mm and the antenna is placed in the center of the turntable to test its far-field pattern. The receiving probe is the same Vivaldi antenna, fixed on the platform, 6000 mm ($100\lambda 0$) away from the center of the antenna under test, and in the same horizontal plane as the antenna under test. The antenna to be tested is in the transmitting state. Using the antenna far-field measurement system composed of a signal source and vector network analyzer, the turntable is rotated 360° and sampled at 1° intervals to obtain the far-field pattern of the azimuth plane of the antenna under test. Then, on the same plane as the antenna, objects are placed that can strongly reflect electromagnetic waves around the antenna to simulate the interference of multi-path effects, such as the metal plate and metal ball used in this experiment, and analyze its influence on the AUT pattern. The modal filtering technology is used to verify its suppression effect on the interference in this non-absorbent environment.

The placement position of the interfering object is shown in Figure 7. Position 1 is located on the left side of the antenna, r2 = 300 mm away from the antenna; position 2 is located 45° in front of the antenna to the right, and the distance from the antenna is r1 = 300 mm. In this experiment, the interfering objects are a metal plate with a diameter of 110 mm × 30 mm and a metal ball with a radius of 140 mm.

Two experiments were designed to verify our conclusions from different frequencies and different interference locations.

1. Experiment I

AUT works at F1 = 4 GHz. The interfering object is a 110 mm × 30 mm ($1.5\lambda 1 \times 0.4\lambda 1$) metal plate, $\lambda 1$ = 75 mm, which is placed on interference position 1 shown in Figure 7, as shown in Figure 8 below. The distance between the probe and the antenna under test is 6000 mm ($80\lambda 1$) and the probe is in the far-field radiation region of the antenna under test. The antenna under test, the probe, and the interfering object are all in the same horizontal plane. Applying the far-field measurement system, the antenna under test rotates with the turntable, starting from 0° and ending at 360°. Samples are taken at an interval of 1° to test the cross-section radiation field pattern of the azimuth plane of the antenna under test.

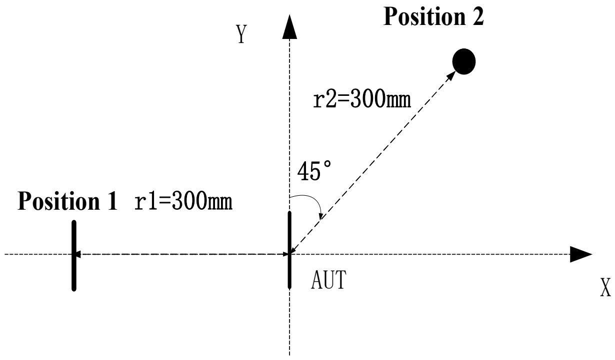

Figure 7. Schematic diagram of the position of the interfering object.

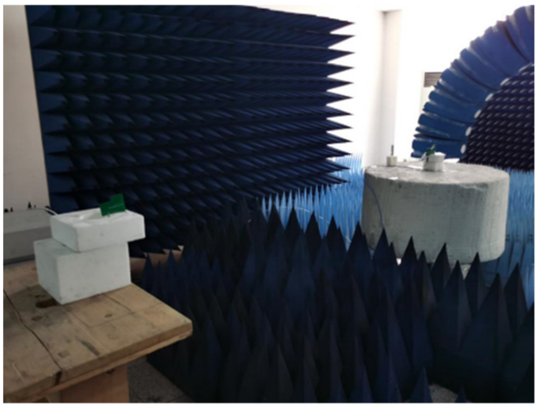

Figure 8. Experiment I test scene.

From the two different test environments of Figures 6 and 8, the pattern E1 of the AUT without interference and the pattern E2 of the metal plate interference are obtained. For the electric field E2 with a multi-path effect, the modal filtering technology is applied to suppress the influence of the metal plate on the AUT test results. If the antenna size and operating frequency are known, the corresponding number of mode items is N1 = [k1 × r0] = 5, k1 = 2π/λ1. Taking the first five items of the spherical wave expansion mode items of the electric field E2, the influence of the metal plate can be suppressed and the accurate antenna measurement pattern E3 after filtering can be obtained. The measurement results are shown in Figure 9 below.

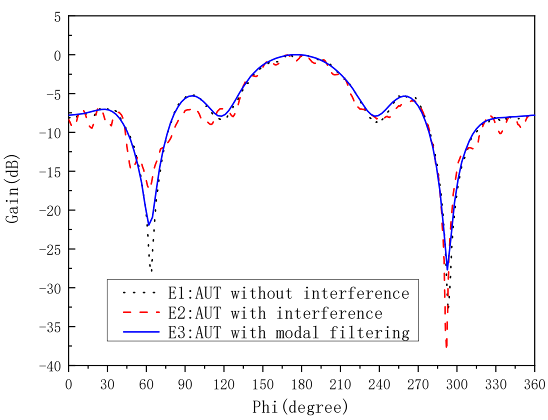

Figure 9. Comparison of the antenna pattern before filtering and after filtering.

It can be seen from Figure 9 that, for the antenna pattern including the reflection interference from the metal plate, the modal filtering technology eliminates the disturbance of the main lobe and the back lobe; 2.5 dB interference is filtered out at the −10 dB level, which greatly improves the measurement accuracy of the antenna.

2. Experiment II

The AUT works at 6 GHz and the interference object is a metal ball with a radius of 140 mm (2.8λ2), λ2 = 50 mm, which is placed on interference position 2 shown in Figure 6, as shown in Figure 10 below. The distance between the probe and the antenna under test is 6000 mm (120λ2) and the probe is in the far-field radiation region of the antenna under test. The experimental equipment and procedure are the same as in Experiment I.

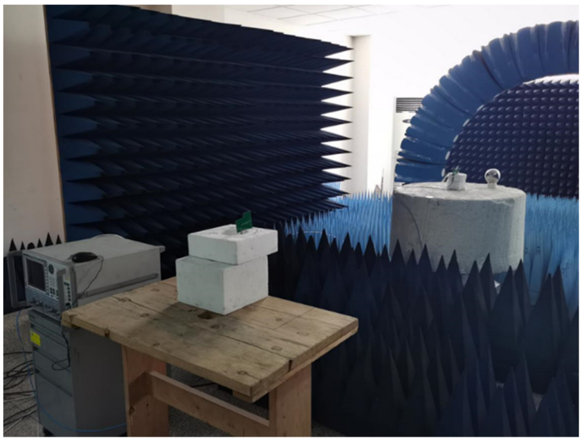

Figure 10. Experiment II test scene.

The processing steps of modal filtering are the same as those of experiment I. In this experiment, the wideband antenna to be tested is at a different operating frequency of 6 GHz, so the number of mode terms corresponding to the smallest spherical wave surrounding the antenna has changed compared with before, N2 = [k2 × r0] = 7, k2 = 2π/λ2. Taking the first seven items in the spherical wave expansion mode items of the interference electric field E4 with the presence of metal balls, the interference can be suppressed and the filtered antenna pattern E5 can be obtained. The analysis and comparison of the antenna pattern E1 without interference, the antenna pattern E4 with metal balls, and the field E5 after modal filtering of the electric field E4 are shown in Figure 11 below.

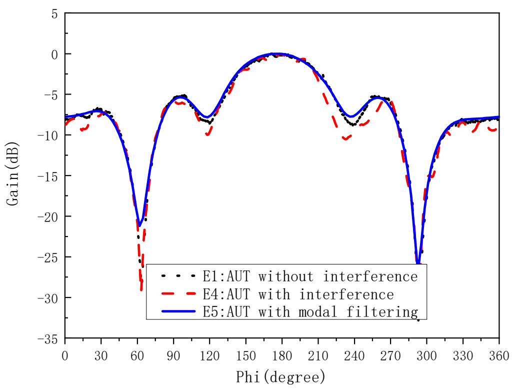

Figure 11. Comparison of the antenna pattern before filtering and after filtering.

It can be seen from Figure 11 that the existence of the metal ball has a great influence on the antenna test, resulting in the distortion of the main lobe, and the overall pattern also has a large error. The modal filtering technology eliminates the interference of the main lobe well, reduces the error in other directions, and filters out 3 dB interference at the −10 dB level, which greatly improves the measurement accuracy of the antenna.

3. Experiment III

The AUT works at 7.5 GHz and the interference object is a dihedral angle structure with two metal plates perpendicular to each other. The size of the metal plate is 200 mm × 200 mm ($5\lambda3 \times 5\lambda3$), $\lambda3$ = 40 mm, which is placed on interference position 2 shown in Figure 6. As shown in Figure 12 below, the distance between the probe and the antenna under test is 6000 mm ($150\lambda3$) and the probe is in the far-field radiation region of the antenna under test. The experimental equipment and procedure are the same as in Experiment I.

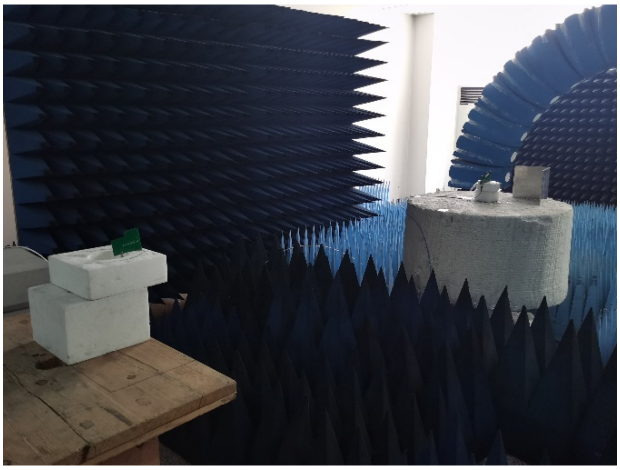

Figure 12. Experiment III test scene.

The processing procedure of modal filtering is the same as in experiment I. In order to verify the broadband characteristics of the method, the operating frequency of the antenna under test is set as 7.5 GHz and the wavelength is $\lambda3$ = 40 mm in this experiment. At this time, the radius of the minimum sphere surrounding the antenna remains the same, r0 = 52.2 mm. Owing to the change in the working frequency, the corresponding number of mode terms has changed, N3 = [k3 × r0] = 8, k3 = $2\pi/\lambda3$. Taking the first eight items in the spherical wave expansion mode items of the interference electric field E6 with the presence of the metal dihedral angle structure, the interference can be suppressed and the filtered antenna pattern E7 can be obtained. The analysis and comparison of the antenna pattern E1 without interference, the antenna pattern E6 with the metal dihedral angle structure, and the field E7 after modal filtering of the electric field E6 are shown in Figure 13 below.

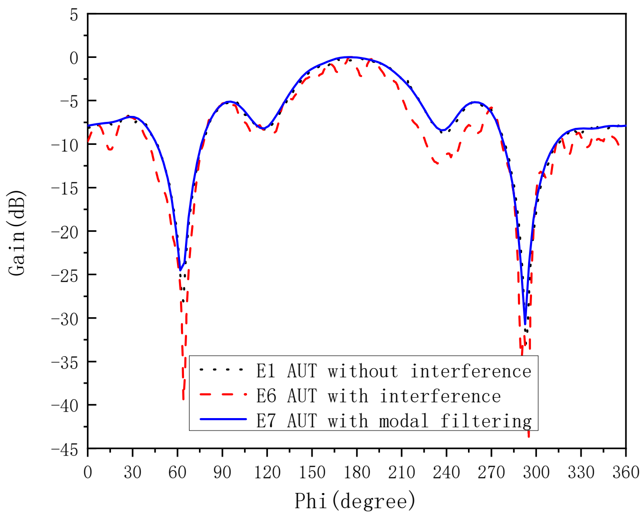

Figure 13. Comparison of the antenna pattern before filtering and after filtering.

As can be seen from Figure 13, owing to the strong reflection characteristic of the metal dihedral angle structure, the interference caused by its large surface area brings huge interference level superposition in the antenna measurement results, leading to complete deformation of the main lobe and a maximum error of 5 dB on the side lobe. This kind of huge error is completely caused by the artificial introduction of the external strong interference source. In actual measurement, this kind of strong interference source should be avoided first. The mode filtering method can eliminate the interference of the main lobe, recover the shape of the main lobe, and correct the errors in other directions. In the main lobe range, at the 0 dB level, it filters out 3 dB interference. In the side lobe range, 5 dB interference is filtered at the −10 dB level, which greatly improves the measurement accuracy of the antenna.

The above three experiments with different operating frequencies (4 GHz, 6 GHz, and 7.5 GHz) show that pattern filtering technology is not sensitive to frequency. When operating at different frequencies, the corresponding operating wavelength changes, resulting in a change in the number of mode items required by the minimum ball surrounding the antenna. At different frequencies, this method can be used to suppress reflection interference by selecting a different number of mode items, without additional operation and calculation. It is very suitable and applied to broadband antenna measurement to suppress interference in the non-absorbent measurement of wideband antennas and to obtain more accurate measurement results independent of site.

5. Conclusions

In wideband antenna non-absorbent measurement, it is a simple and effective method to apply modal filtering technology to reduce the interference of multi-path effects and improve the measurement accuracy. The modal filtering technology has no limit to the operating frequency in theory. It is suitable for the measurement of wideband and even ultra-wideband antennas. No additional testing steps are required during the measurement. Only the dimensional data of the antenna are required, which are known in most cases. The numerical simulation and actual test results show that modal filtering technology has an obvious suppression effect on multi-path interference, and the test can even be carried out in a non-absorbent environment, which greatly improves the measurement accuracy and reduces the equipment requirements.

Author Contributions: Conceptualization, S.G.; Data curation, Y.S.; Formal analysis, Y.S.; Investigation, Y.S.; Software, Y.S.; Supervision, S.G.; Writing—original draft, Y.S.; Writing—review & editing, Y.S. and S.G.; All authors have read and agreed to the published version of the manuscript.

Funding: This research received no external funding.

Conflicts of Interest: The authors declare no conflict of interest.

References

1. Kang, J.S.; Park, J.I.; Kim, J.H. Antenna Measurement Comparison of 700–1100 MHz/R-/X-band Horn Antennas. In Proceedings of the 2018 International Symposium on Antennas and Propagation (ISAP), Busan, Korea, 23–26 October 2018; pp. 1–2.
2. Jain, S.K.; Jain, S. Error and uncertainty estimation in gain measurement of double ridge horn antenna working for 1–18 GHz. *Int. J. Syst. Assur. Eng. Manag.* **2022**, *13*, 1497–1507. [CrossRef]
3. Hess, D.W. A theoretical description of the IsoFilter(TM) rejection curve. In Proceedings of the 5th European Conference on Antennas and Propagation (EUCAP), Rome, Italy, 11–15 April 2011; pp. 3892–3896.
4. Gregson, S.F.; Parini, C.G.; Newell, A.C. A General and Effective Mode Filtering Method for the Suppression of Clutter in Far-Field Antenna Measurements. In Proceedings of the 2018 AMTA Proceedings, Williamsburg, VA, USA, 4–9 November 2018; pp. 1–5.
5. Gemmer, T.M.; Heberling, D. Accurate and Efficient Computation of Antenna Measurements Via Spherical Wave Expansion. IEEE Trans. *Antennas Propagat.* **2020**, *68*, 8266–8269. [CrossRef]
6. Gregson, S.F.; Tian, Z. Verification of Generalized Far-Field Mode Filtering Based Reflection Suppression Through Computational Electromagnetic Simulation. In Proceedings of the 2020 IEEE International Symposium on Antennas and Propagation and North American Radio Science Meeting, Montreal, QC, Canada, 17 February 2021; pp. 2059–2060. [CrossRef]

7. Hindman, G.E.; Newell, A.C. Reflection Suppression in a large spherical near-field range. In Proceedings of the AMTA 27th Annual Meeting & Symposium, Newport, RI, USA, 18–20 October 2005.
8. Hindman, G.E.; Newell, A.C. Reflection Suppression to Improve Anechoic Chamber Performance. *AMTA Eur.* **2006**, *2006*, 297–302.
9. Gregson, S.F.; Newell, A.C.; Hindman, G.E. Reflection Suppression in Cylindrical Near-Field Antenna Measurement Systems—Cylindrical MARS. In Proceedings of the AMTA 31st Annual Meeting & Symposium, Salt Lake City, UT, USA, 23–25 November 2009.
10. Gregson, S.F.; Newell, A.C.; Hindman, G.E.; Carey, M.J. Advances in cylindrical Mathematical Absorber Reflection Suppression. In Proceedings of the Proceedings of the Fourth European Conference on Antennas and Propagation, Barcelona, Spain, 12–16 April 2010; pp. 1–5.
11. Gregson, S.F.; Newell, A.C.; Hindman, G.E.; Carey, M.J. *Extension of the Mathematical Absorber Reflection Suppression Technique to the Planar Near-Field Geometry*; AMTA: Atlanta, GA, USA, 2010.
12. Gregson, S.F.; Newell, A.C.; Hindman, G.E.; Carey, M.J. Application of Mathematical Absorber Reflection suppression to planar near-field antenna measurements. In Proceedings of the Proceedings of the 5th European Conference on Antennas and Propagation (EUCAP), Rome, Italy, 11–15 April 2011; pp. 3412–3416.
13. Boehm, L.; Foerstner, A.; Hitzler, M.; Waldschmidt, C. Reflection Reduction Through Modal Filtering for Integrated Antenna Measurements Above 100 GHz. *IEEE Trans. Antennas Propag.* **2017**, *65*, 3712–3720. [CrossRef]
14. Gregson, S.F.; Tian, Z. Comparison of Spherical and Cylindrical Mode Filtering Techniques for Reflection Suppression With mm-wave Antenna Measurements. In Proceedings of the 2018 IEEE Conference on Antenna Measurements & Applications (CAMA), Västerås, Sweden, 3–6 September 2018; pp. 1–4. [CrossRef]
15. Eichenberger, J.; Yetisir, E.; Ghalichechian, N. High-Gain Antipodal Vivaldi Antenna with Pseudoelement and Notched Tapered Slot Operating at (2.5 to 57) GHz. *IEEE Trans. Antennas Propag.* **2019**, *67*, 4357–4366. [CrossRef]
16. Liang, J.C.; Chiu, C.N.; Lin, T.C.; Lee, C.H. An Ultrawideband Circularly-Polarized Vivaldi Antenna with High Gain. *IEEE Access* **2022**, *10*, 100446–100455. [CrossRef]
17. Hansen, J.E. Scattering matrix description of an antenna. In *Spherical Near-Field Antenna Measurements*; Peter Peregrinus Ltd.: London, UK, 1988.
18. Tian, Z.; Gregson, S.F. Examination of Spherical Antenna Far-Field Scattering Suppression Through Electromagnetic Simulation. In Proceedings of the Antennas and Propagation Conference, Birmingham, UK, 11–12 November 2019.
19. Tian, Z.; Gregson, S.F. Examination of the Effectiveness of Mode Orthogonalization and Filtering for Scattering Suppression in Antenna Measurements Through Computational Electromagnetic Simulation. In Proceedings of the European Conference on Antennas and Propagation, Krakow, Poland, 31 March–5 April 2019.
20. Jensen, F.; Frandsen, A. On the number of modes in spherical wave expansions. In Proceedings of the AMTA 26th Annual Meeting & Symposium, Stone Mountain Park, GA, USA, 17–22 October 2004.